electronics

MDPI

Article

The Implementation of a High-Frequency Radio Frequency Identification System with a Battery-Free Smart Tag for Orientation Monitoring

Tilen Svete *, Nejc Suhadolnik and Anton Pleteršek

STMicroelectronics d.o.o., Tehnološki Park 21, 1000 Ljubljana, Slovenia; nejc.suhadolnik@st.com (N.S.); anton.pletersek@st.com (A.P.)

* Correspondence: tilen.svete@st.com; Tel.: +386-41-383-974

Academic Editors: Ali Shemshadi and Michael Sheng

Received: 19 September 2016; Accepted: 28 December 2016; Published: 4 January 2017

Abstract: Energy-harvesting passive RFID (radio frequency identification) tags provide countless possibilities as so-called smart tags. Smart tags can communicate with existing RFID readers or interrogators while providing a battery-less platform for internal and external sensors to enrich available information about the environment and smart tag it. A reduced cost and size as well as an increased lifespan and durability of battery-free smart tags offer improvements in areas such as transportation and product tracking. Battery-free smart tags can ideally support arbitrarily complex sensor measurements, but in reality energy limitations can introduce great reductions in operating range and thus application range. In this work, we present an example application of a smart tag with a passive HF (high-frequency) RFID tag IC (integrated circuit) and MEMS (micro electro-mechanical structure) sensor. A standard HF RFID reader connected to a PC (personal computer) allowed the RF (radio frequency) field to power and communicate with the smart tag. A Kalman filter, implemented on a PC, was used to correct and improve the raw sensor data of smart tag orientation. Measurement results showed that the MEMS sensor on the smart tag could be powered for continuous operation and that raw smart tag orientation data could be read while in the RF field of a standard HF RFID reader, but at a limited range.

Keywords: RFID; contactless sensor; data logging; energy harvesting; Kalman filter; smart tag

1. Introduction

Passive RFID tags are devices that receive power for operation from the RF field generated by a reader. They act as slaves in reader-tag communications. The reader issues commands by amplitude modulation of the RF field, to which passive tags respond by modulating the load of their antenna to induce a change in RF field amplitude or phase. This change is received by the reader. Due to their passive nature, they do not require a battery for operation, which increases their life span and reduces their size and cost. As such, they have good reliability and have a wide variety of applications such as product tracking and data storage.

The area of RFID is very broad, with LF (low frequency), HF (high frequency), and UHF (ultra-high frequency) forming the bulk of the market in passive tags. Carrier frequencies for LF range from 30 kHz to 300 kHz, with most tags operating at 125 kHz. For HF, the frequency range is from 3 MHz to 30 MHz, with the majority of tags operating at 13.56 MHz—the example presented in this paper included. UHF carrier frequencies range from 300 MHz to 3 GHz, with the most common band being from 860 MHz to 960 MHz. Operating ranges for LF and HF RFID tags are up to 10 cm (up to 1 m for HF vicinity cards) due to inductive coupling of antennas for power transfer, and over 10 m for UHF tags, due to the electromagnetic coupling of antennas.

Passive tags require very little power for operation. At smaller distances, the reader RF field can be much stronger than what is required to power the tag. This excess power can be utilized by employing energy harvesting to charge batteries or power other devices, such as sensors. External sensors attached to an energy harvesting tag improve upon the basic tag functionality of wireless communication and data storage in many ways, depending on sensor and application.

RFID tag ICs can also include ports for wired communication, enabling it to communicate with other ICs. A tag IC can in this case act as an interpreter between wired and wireless communication. Tag ICs like this then become building blocks for so-called smart tags or smart active labels (SAL). Smart tag is a term for devices that include an RFID tag for wireless communication and power supply, and other ICs, such as MCUs, sensors or additional external memory ICs. Similar are smart active labels, which can also denote ICs with RFID capabilities as well as integrated sensors (e.g., an integrated temperature sensor), a power management unit, and wired communication capability. In the case of an added battery, the power management unit can charge the battery while the RF field is present, while the battery provides power when the RF field is not present. Other ICs connected to the smart active label can thus be powered and their data logged even if the RF field is not present, providing the battery has enough charge. Smart tags and smart active labels build on the advantages of RFID tags by vastly increasing potential applications. The implementation of the so-called Internet of Things (IoT) strongly benefits from smart tags and smart active labels.

In recent years, numerous papers have shown that the battery-free sensing of environmental data such as light, humidity, and pressure with passive RFID smart tags or smart active labels is feasible and offers new opportunities in areas such as transportation and product tracking, agriculture plant monitoring [1], weather and environmental parameter logging [2], medical research [3], and more. This paper expands on the above examples by presenting an HF RFID system for data logging, measurements, and power transfer over a short distance. Also presented is a battery-less smart tag capable of executing simple preprogrammed commands, eliminating the need for an onboard MCU, and providing sufficient power for continuous power intensive measurements by the onboard sensor.

A challenge in battery-free RFID-based sensor applications is a power supply for sensor operation and data logging. Depending on the sensor, the power requirements for performing measurements can become quite large, relative to tag power consumption. There are two approaches to ensuring there is enough power for sensor operation during measurements. The first is to constantly have a strong enough RF field present to power the sensor while it performs continuous measurements—what the example in the paper uses. The second is to store energy from the RF field on a capacitor to provide enough energy for the sensor to perform a single measurement and for the passive tag to store the result and transmit it back to the reader.

In this paper, we provide an example application of an HF RFID smart tag, consisting of a passive HF RFID tag IC and MEMS IC with an integrated multi-axis accelerometer and gyroscope. Raw sensor data from smart tag orientation measurements were merged and enhanced using a Kalman filter [4], implemented on a PC (personal computer). A standard HF RFID reader completed the link between the PC and the MEMS sensor onboard the smart tag.

In this example, four key points are brought to light. First and second are the wireless data and the power transfer from the reader to the smart tag. Third is the passive tag IC with the ability to execute simple commands to communicate with the MEMS sensor, without the need for an MCU on the smart tag, reducing cost and power demand. Lastly is the data processing on a PC to extract the most information out of the available raw sensor data.

Section 2 describes the AS39514 HF RFID passive tag IC, its capabilities, digital interface, and energy harvesting. Section 3 describes the MPU 6050 [5] multi-axis accelerometer and gyroscope integrated circuit, its power requirements, digital interface, and sensing capabilities. Section 4 describes the Kalman filter used for raw sensor data merging and enhancing. In Section 5, an example application of a short-range wireless bridge utilizing the AS3911 HF RFID reader [6] and AS39514 passive tag to power and sample the MPU 6050 multi-axis accelerometer and gyroscope is described. Results of the

wireless bridge performance and Kalman filter operation are presented in Section 6. Possible uses of such a wireless bridge are discussed in Section 7.

2. Smart Tag with I²C and SPI Interface and Energy Harvesting

Smart active labels or smart tags offer contactless communication with RFID readers and fall into two main categories. The first being HF RFID devices, which are compliant with standards ISO/IEC 14443 type A/B, ISO/IEC 15693, and JIS X 6319-4 (FeliCa). The second being UHF RFID devices, which are compliant with standard ISO/IEC 18000-6 and EPCglobal Gen2. The commands and protocols defined by these standards are built into tag ICs.

The passive tag IC AS39514 is designed for use in smart dual protocol RFID tags based on contactless proximity or vicinity communication. It supports passive operations at 13.56 MHz and is NFC-F (FeliCa) Type 3 tag and ISO/IEC 15693 compliant. The IC includes a serial communication interface for SPI (serial peripheral interface) or I²C (inter integrated circuit) port to easily connect to digital sensors, serial memory devices, or microcontrollers. Figure 1 shows the internal blocks of the IC and how the connect to the pins.

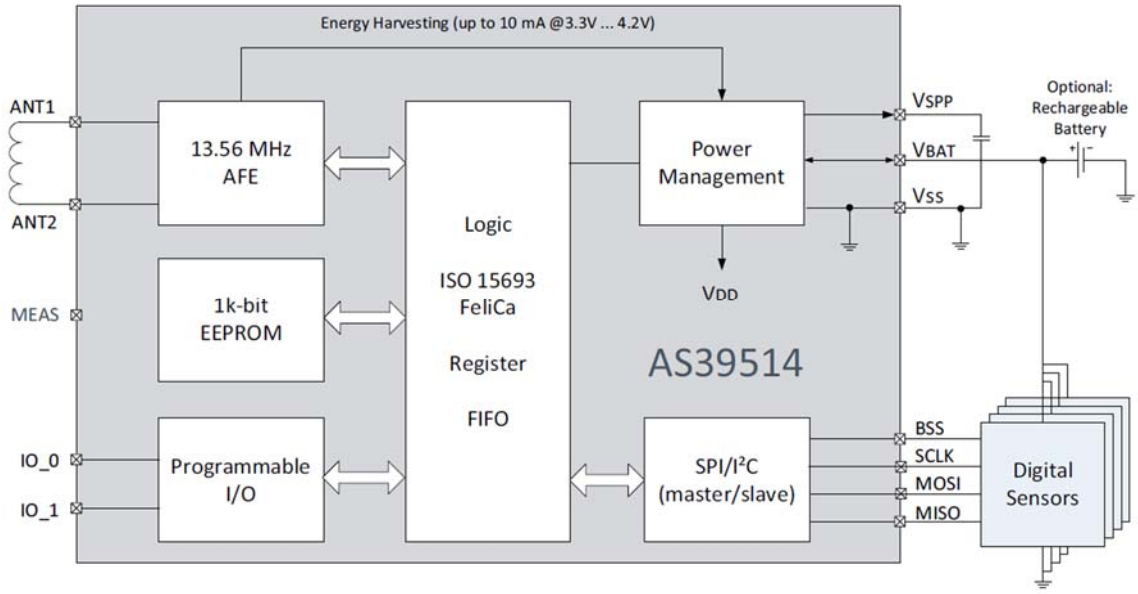

Figure 1. AS39514 passive tag IC block schematic.

The on-chip power management harvests energy from the RF field to supply external devices, or to charge a rechargeable battery or capacitor. It can supply currents up to 10 mA (at 3.3 V) and voltages up to 4.2 V.

The AS39514 can be configured to act as an I²C master between itself and up to four external digital sensors. The interface is programmable with a micro-program that is loaded into the on-chip EEPROM (electrically erasable programmable read-only memory) or can be dynamically loaded into the FIFO (first in first out) buffer by an HF RFID reader. The I²C master operation can be programmed with a simple hardware language that has some defined commands, as shown in Table 1 below. This enables the AS39514 to issue simple commands to read and write sensors without the need for an MCU (microcontroller unit) on the smart tag. The micro code in this case contained only two I²C write commands to enable the sensor and continuous measurements, and a single 14-byte I²C read command to read data from all three accelerometers, all three gyroscopes, and the temperature sensor integrated with the MEMS sensor (2 bytes per axis and temperature, for a total of 14 bytes). All registers containing data are arranged in a sequential manner, so one I²C read command was enough to access all required data.

Table 1. List of micro-program commands (shortened), available to the user.

Code #	Instruction Code								Instruction Function
	Bit #								
	7	**6**	**5**	**4**	**3**	**2**	**1**	**0**	
1	0	0	0	0	S3	S2	S1	S0	Enable output drivers (enable and battery power output) – S3 = driver 3, S2 = driver 2, S1 = driver 1, S0 = driver 0
2	0	1	T5	T4	T3	T2	T1	T0	Delay time in 10 µs steps (e.g., 000101 = 50 µs)
3	1	0	T5	T4	T3	T2	T1	T0	Delay time in 1 ms steps (e.g., 000101 = 5 ms)
4	1	1	0	0	0	0	0	0	NOP (no operation)
5	1	1	0	0	0	0	0	1	I^2C start condition
6	1	1	0	0	0	0	1	0	Reserved
7	1	1	0	0	0	0	1	1	I^2C stop condition
8	1	1	0	1	N3	N2	N1	N0	I^2C write command – generates Start condition, I^2C slave address + W bit, N number of bytes. The N value defines how many bytes are following the I^2C write command and are regarded as RAW data.
9	1	1	1	0	N3	N2	N1	N0	I^2C read command – generates Start condition, I^2C slave address + R bit, N number of bytes. The N value defines how many bytes will be read out of the I^2C device. The received bytes are stored in the FIFO buffer to be read out by the RFID reader.
...									...
14	1	1	1	1	1	1	1	1	End of sequence

3. Multi-Axis Accelerometer and Gyroscope

The MEMS sensor MPU 6050 contains a 3-axis accelerometer and a 3-axis gyroscope, which consume a relatively large amount of power during operation. It consumes 3.8 mA in typical conditions when all three axes of the gyroscope and all three axes of the accelerometer are enabled and performing measurements. The sensor can act as an I^2C master for other slave sensors, such as magnetometers. In addition, it houses a Digital Motion Processor for advanced data processing on the sensor itself to reduce the computational load on the MCU controlling it.

The gyroscope has a user-programmable full-scale range of ± 250, ± 500, ± 1000, and $\pm 2000^\circ/s$, while the accelerometer has a user-programmable full-scale range of ± 2 g, ± 4 g, ± 8 g, and ± 16 g [5]. Each axis of the gyroscope and accelerometer has its own 16-bit analog-to-digital converter (ADC), for a total of six ADCs. It supports I^2C communication up to 400 kHz.

4. Kalman Filter

The Kalman filter [4,7,8] is a recursive algorithm that uses measurements over time—in this example, measurements of a gyroscope and accelerometer—to estimate the state of a process by minimizing the mean of the squared error. The states of the measured system—in this example, the angle or orientation and the bias of the angle of the smart tag—are hidden to us, and only the measured output is available (value measured by the sensor). This is also known as a hidden Markov model. The sensor measurements include noise that, at a constant smart tag angle, produces multiple measured values with a probabilistic distribution. The filter attempts to estimate a more accurate current state of the system, based on the past estimated state and current measurements, than one could attain from accelerometer or gyroscope measurements alone.

In this example, the errors of the sensors are as follows. The accelerometer is in essence very noisy and can produce a very erroneous measurement if read only once. However, in the long term, accelerometer measurements are very reliable. Coincidentally, the gyroscope has inverted characteristics. When read once, the angular velocity data is very reliable. The measured values include some offset error. When these angular velocities with a small offset are integrated in regard to

time, they exhibit drift. In the long term, the integrated gyroscope data is not reliable. To summarize, the gyroscope data is reliable in the short term and accelerometer data is reliable in the long term.

Accelerometer and gyroscope data is used in the following way. Three accelerometers for all three axes (X, Y, and Z) are used to determine the orientation of the smart tag (pitch, roll, and yaw). These are the measurements of the state of the system. Gyroscope measurements, for rotation around the three axes, provide the angular velocity, or the rate of angle change. When integrated with respect to time, an angle can be obtained from the angular velocities. Gyroscope measurements are used as a base point to predict the next system state, while accelerometer measurements are used to update the estimate of the state of the system. The estimate of the state of the system is the last estimate of the state with an added difference between the accelerometer measurement and prediction (multiplied by the Kalman gain, it holds information about the variances of the measurements). The variances of the measurements determine how much we trust either the gyroscope measurements or the accelerometer measurements.

5. Example Application

In our example, the HF RFID reader IC AS3911 and passive tag IC AS39514 formed a short-range wireless bridge for communication and power transfer. The bridge provided a link between a PC and the multi-axis accelerometer and gyroscope sensor MPU 6050. The AS3911 reader IC was part of a demo reader PCB. The demo reader PCB was connected to a PC via USB (universal serial bus). Communication between the reader and tag was done via FeliCa protocol at a data rate of 424 kbit/s. The passive tag IC AS39514 was part of a smart tag PCB, which also included an antenna and MPU 6050 sensor. Communication between AS39514 and MPU 6050 was done via I^2C protocol at 400 kHz. The dimensions of the reader antenna were 65 mm $\times$ 65 mm with 2 coil turns. The tag antenna was a standard Class 1 antenna, as defined by ISO/IEC 10373-6, which measures 71.5 mm $\times$ 41.5 mm with 4 coil turns.

Figure 2 shows the basic components of the setup. The AS3911 demo PCB includes the HF RFID reader IC AS3911, an antenna, and an MCU to, among other tasks, convert USB commands from the PC into SPI commands that the AS3911 understands. The reader drives the antenna to provide any tags within its RF field with power and a medium for communication. The smart tag antenna is inductively coupled to the reader antenna, in essence forming a transformer. The coupling factor between the coils of the two antennas is determined by the distance between them. Communication between the reader and tag takes place over this HF RF field, with the reader emitting AM (amplitude modulated) signals and the tag returning signals via passive load modulation of its antenna. The reader can detect these replies as either AM or PM (phase modulation), depending on the reader-tag antenna system and its surroundings. The smart tag draws the power for its operation from this RF field. This means that the power available to the smart tag drops as the distance between the two antennas is increased. The passive tag IC AS39514 included on the smart tag has a built in energy harvesting circuit, which uses the RF field to power any sensors, batteries, or other devices that are connected to it. The passive tag IC does not use much power for itself, so any excess power available on the tag antenna can be used for energy harvesting purposes. Using the AS39514 micro-program feature, the MEMS sensor data could be read via I^2C protocol without the need for an MCU on the smart tag PCB, thus eliminating a component in need of powering and reducing the cost of the smart tag.

On the PC, the measured data was further enhanced by using a Kalman filter. The algorithm was realized in a powerful computational program Scilab. While smart tag orientation can be determined from accelerometer data alone, fusing accelerometer and gyroscope data using a Kalman filter gives greater precision and accuracy. The cost for this is an increased power supply for the smart tag and an increased price of the MEMS sensor.

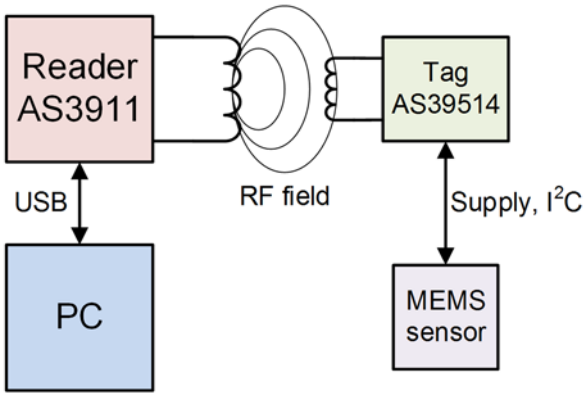

Figure 2. Block diagram of the measurement setup.

The total computational requirements for the Kalman filter for one time step are 12 multiplications, 2 divisions, 5 additions, and 10 subtractions. Because we used a PC to compute the filter results, computational complexity was not an issue. However, the filter could be implemented on an MCU to compute the filter output in real time [9]. The MCU controlling the reader IC could be used to additionally compute the filter equations while not busy with other tasks.

The sensor continuously performed measurements while in the reader RF field. Data was read about 3 times per second and stored on the PC for later evaluation. The micro-program was split into two parts: the sensor initialization part and the data read part. The MEMS sensor, when enabled, takes about 30 ms to begin measurements. For this reason, the initialization command was sent first, followed by repeating the data read command to access new data. An example micro-program code to enable the MPU 6050 (wake it up from a sleep state) is 0x01 0xD2 0x6B 0x00 0xC3. Using Table 1, we can quickly decode this into the following steps: enable output driver for communication, I^2C write command for two bytes (takes next two bytes as raw data), sensor register address, data to be written, and I^2C stop condition. This code is written into the EEPROM of the AS39514 beforehand and executed by using the "Access FIFO" custom FeliCa command of the AS39514 with service code bytes set to 0xAF 0x42. These two bytes define that stored sequence 2 (from the lower nibble of the second byte) must be executed. To execute a different sequence, the lower nibble would be set to a different number (4 total sequences, so from 1 to 4).

The I^2C read command for 14 bytes had a similar format and was also stored into the EEPROM beforehand. When it was executed using the aforementioned custom command, the data read via I^2C was stored into the FIFO buffer of the AS39514. To retrieve this data from the smart tag, the "Access FIFO" command was used again, but with different service code bytes. In this case, the bytes would be 0xAF 0x8E to read 14 bytes from the FIFO buffer.

6. Results

The wireless bridge, connecting the reader and smart tag, was able to power the MEMS sensor during measurements. The sensor has a minimal supply voltage of 2.375 V and requires 3.8 mA of current if all three accelerometers (one per axis) and all three gyroscopes (again, one per axis) are running continuously. At a distance of 2 mm, with the antennas in a concentric configuration, the AS39514 was able to provide 3 V and 4 mA to the sensor. With all accelerometer and gyroscope axes always enabled and performing measurements, the maximum distance achieved was 1 cm. At larger distances, the coupling factor between the reader and tag antenna became too small and not enough power was delivered to the MEMS sensor for reliable continuous operation.

Prior to measurements the sensor was not calibrated. Calibration reduces the offset or bias in angular velocity data, which in turn reduces drift when angular velocity is integrated. No calibration meant that the drift in angle values would be very apparent. In turn, filter operation in removing said

drift would be very apparent as well, as can be seen in Figure 3. In mass production, precise calibration of such sensors may not be feasible for various economic reasons.

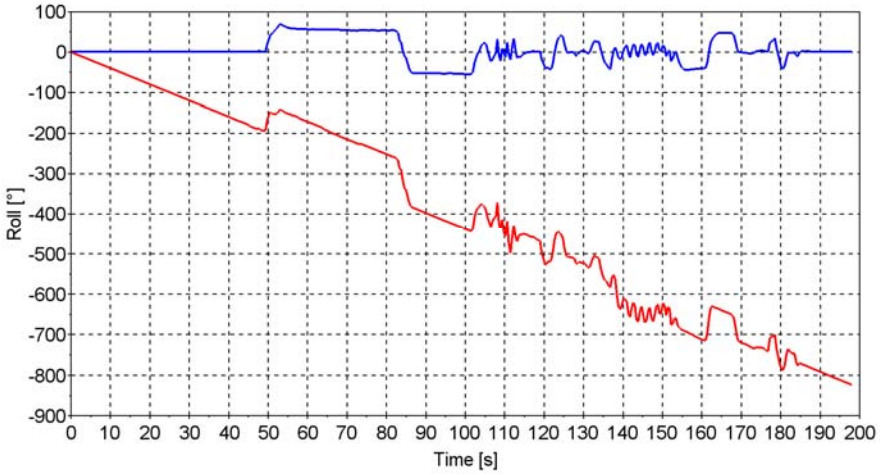

Figure 3. Integrated raw gyroscope data in red and Kalman filter output in blue during example orientation changes of the smart tag roll. We can observe a large drift in integrated gyroscope data while the filter output shows no drift.

The standard deviation of integrated gyroscope data for the pitch of the smart tag, with bias removed, when the sensor was stationary was 0.165° with a mean value of −1.411° (0° representing horizontal orientation). Similarly, the standard deviation of the accelerometer data when the sensor was in a stationary orientation was 0.176°, with a mean of 0.376°. The Kalman filter output showed reduced standard deviation, only 0.114°, with a mean of 0.375°. The pitch of the smart tag, measured by hand, was approximately 0.4°. These results show that the Kalman filter does indeed provide a better estimate of the state of a system than one could attain from measurements alone. Some additional results from the tag roll measurements are shown below in Table 2. The measurements were taken over a span of 10 to 30 s while the tag was stationary.

Table 2. Comparison of the standard deviation (and mean value) of the tag roll measurements.

Accelerometer	Gyroscope	Kalman Filter
0.218° (1.248°)	0.229° (−1.303°)	0.158° (1.244°)
1.399° (55.049°)	1.332° (52.635°)	1.259° (55.000°)
0.576° (−52.901°)	0.495° (−55.142°)	0.355° (−52.825°)

We can observe an improvement in standard deviation in the Kalman filter results in all three cases.

7. Possible Uses and Discussion

A battery-free UHF smart tag employing energy harvesting to charge a supercapacitor to power a small camera was presented in [10]. The work showed that high-energy loads can be powered for single sample measurements and data transfer, without the need for a costly onboard battery. The example in our work could be improved in a similar manner, by employing a supercapacitor to power the MEMS sensor for single measurement operation and data transfer or logging.

One of the possible uses of smart tags with orientation and shock sensing is in so-called smart storage racks for stored item monitoring. Smart storage racks or smart shelves are shelves with antennas built into them to power RFID smart labels attached to stored items [11]. A smart tag with multiple sensors attached to the item could track its state (temperature, moisture, orientation, shock,

etc.) and provide valuable information about its current and past state to all parties involved in the transportation or storage process.

Another use of short-range wireless power and data transfer for measurement purposes is in places such as vacuum chambers or rotating platforms, where wired connections are not practical or even not possible. In the former case, we can give an example of an experiment in a vacuum chamber. Because of the vacuum chamber design, sensors inside the chamber may not be accessible with wires. Antennas could be attached to each end of the chamber window, providing both power and data transfer for sensors inside the chamber, while also still permitting human observations through the window.

In the case of rotating platforms, any wires can become tangled in the shaft of the device, or in the case of a circular armature, become worn over time or lose contact in some other way. Again, attaching two antennas, one to the base and one to the rotating platform (concentric or in such a way that coupling factor remains constant regardless of rotation), would provide a solution to this problem. In the case of a circular armature, an additional benefit would be the removal of contact brushes, increasing reliability and life span of the measurement setup. Any sensors on the rotating platform could thus be powered and their data read through the antenna setup.

8. Conclusions

We presented an HF RFID battery-free smart tag with MEMS sensor, composed of a multi-axis accelerometer and gyroscope integrated circuit. We have shown that a standard HF RFID reader could power and transfer data to and from the smart tag, even during continuous energy-intensive sensor measurements. While the operating range was very small, we also presented other works that improve energy management and operating range, by storing the required energy for sensor measurement on a supercapacitor, but at the cost of a reduced data logging rate.

We presented an example of a smart tag with a MEMS sensor and without an MCU, thus reducing the number of components on the smart tag as well as reducing power consumption during operation.

We enhanced the gathered data with a Kalman filter, implemented on a PC in a freely available computational program Scilab. The filter merged gyroscope and accelerometer data, and provided a better estimate of the tag orientation than measurements alone could. Such an approach removed any complex computational needs for algorithm calculation from the smart tag and moved them to the PC, where data was stored and evaluated without impacting smart tag performance.

Author Contributions: T.S. conceived and designed the example presented in this paper, performed the measurements, wrote the Kalman filter algorithm, analyzed the measurement and filter data, and wrote the paper. N.S. contributed the tools for communicating with AS39514 and wrote the micro program that was used for communication with MPU 6050. A.P. provided invaluable experience and direction in concieving the example as well as writing the paper.

Conflicts of Interest: The authors declare no conflicts of interest.

References

1. Germšek, B.; Pleteršek, A. Radio frequency identification (RFID) in agriculture-food safety and traceability. In *Paper Proceeding of AgriAnimal, Proceedings of the 2013 International Conference on Agricultural and Animal Sciences, The Sri Lanka Foundation Institute, Colombo, Sri Lanka, 8–9 July 2013*; International Center for Research and Development: Colombo, Sri Lanka, 2013; pp. 30–41.
2. Suhadolnik, N.; Svete, T.; Pleteršek, A. Enhanced Environment Interaction with Use of RFID Smart Labels. *Sens. Transducers J.* **2016**, *197*, 28–33. Available online: http://www.sensorsportal.com/HTML/DIGEST/february_2016/Vol_197/P_2795.pdf (accessed on 3 March 2016).
3. Yeager, D.J.; Holleman, J.; Prasad, R.; Smith, J.R.; Otis, B.P. NeuralWISP: A Wirelessly Powered Neural Interface with 1-m Range. *IEEE Trans. Biomed. Circuits Syst.* **2009**, *3*, 379–387. [CrossRef] [PubMed]
4. Kalman, R.E. A New Approach to Linear Filtering and Prediction Problems. *J. Basic Eng.* **1960**, *82*, 35–45. [CrossRef]

5. InvenSense Inc. MPU-6000 and MPU-6050 Product Specification Revision 3.4. 2014. Available online: http://www.invensense.com/products/motion-tracking/6-axis/mpu-6050/ (accessed on 15 March 2015).
6. ams AG. AS3911B NFC Initiator/HF Reader IC, version 1.15. 2016. Available online: http://ams.com/eng/Products/Wireless-Connectivity/Readers/AS3911B (accessed on 18 July 2016).
7. Welch, G.; Bishop, G. *An Introduction to the Kalman Filter*; University of North Carolina: Chapel Hill, NC, USA, 2006.
8. How a Kalman Filter Works in Pictures. Available online: http://www.bzarg.com/p/how-a-kalman-filter-works-in-pictures/ (accessed on 12 December 2015).
9. Lauszus, K.S. A Practical Approach to Kalman Filter and How to Implement it. Available online: http://blog.tkjelectronics.dk/2012/09/a-practical-approach-to-kalman-filter-and-how-to-implement-it/ (accessed on 5 April 2015).
10. Naderiparizi, S.; Parks, A.N.; Kapetanovic, Z.; Ransford, B.; Smith, J.R. WISPCam: A Battery-Free RFID Camera. In Proceedings of the 2015 IEEE International Conference on RFID, Tokyo, Japan, 15–17 April 2015; pp. 166–173.
11. Wang, X.; Wang, H.; Wang, G. Distributed High-Frequency RFID Antennas for Smart Storage Racks. In Proceedings of the 2010 Second International Conference on Networks Security, Wireless Communications and Trusted Computing, Wuhan, China, 24–25 April 2010; pp. 472–474.